

Localized mechanical instabilities in electronic structure calculations of silica glass under pressure

Nosakhareorodeoremwanta S. O. Ekunwe and Daniel J. Lacks

Department of Chemical Engineering, Tulane University, New Orleans, Louisiana 70118

(Received 14 May 2002; revised manuscript received 31 July 2002; published 18 December 2002)

Calculations are carried out for silica glass under pressure, using the modified neglect of differential overlap semiempirical electronic structure method. The pressure-volume equation of state exhibits discontinuous changes that coincide with the lowest normal-mode frequency decreasing to zero; these results indicate that mechanical instabilities occur due to the disappearance of local minima on the potential-energy surface. These electronic structure results corroborate previous force field results, and thus strengthen the conclusion that localized mechanical instabilities occur in silica glass under high pressure. The mechanical instabilities lead to localized structural transformations that increase the ion coordination and shift the ring size distribution to smaller ring sizes. The structural transformations proceed by highly cooperative rigid unit modes, in which SiO_4 tetrahedra rotate and translate with little internal distortion.

DOI: 10.1103/PhysRevB.66.212101

PACS number(s): 91.60.Gf, 61.43.Fs

Silica glass undergoes interesting transformations at high pressure. Samples compressed to high pressure (>8 GPa) and then decompressed back to atmospheric pressure are irreversibly densified by up to 20%;¹⁻³ the densified glass has been called a distinct amorphous phase of silica.² Also, at high pressure the average silicon coordination number increases gradually from four to six,⁴⁻⁶ and the ring size distribution shifts to smaller ring sizes.⁴ These transformations occur at room temperature, in contrast to the high temperatures necessary for analogous phase transitions and coordination changes in crystalline silica.

Based on a phenomenological model⁷ and molecular simulations,⁸⁻¹⁰ it has been suggested that these pressure-induced transformations in silica glass arise from disappearances of local minima and barriers on the potential-energy landscape, as shown schematically in Fig. 1. After the disappearance of the local energy minimum that the system is in, the system becomes mechanically unstable and is forced to an alternate energy minimum. The structural rearrangements caused by these mechanical instabilities lead to changes in ion coordination and irreversible densification in silica glass. These transformations will occur even at low temperature because thermal activation is not necessary for structural rearrangements caused by a mechanical instability; note that room temperature is considered a “low temperature” for silica, since it is far below the glass transition temperature of silica [~ 1500 K (Ref. 11)]. The significance of these double-well potentials in silica has also been discussed in other contexts.¹²

The previous simulations that showed mechanical instabilities in silica glass under pressure⁸⁻¹⁰ were based on energy calculations using a force field, i.e., a simple function parametrized to give the energy as a function of atomic configuration. The present paper uses an electronic structure method to evaluate the energy of silica glass, in order to determine whether the conclusions regarding the mechanical instabilities are merely artifacts of the force field method. The present paper also examines in detail the nature of the structural rearrangements that accompany the mechanical instabilities.

The simulations are carried out for a system composed of 32 silicon ions and 64 oxygen ions, in a cubic simulation cell with periodic boundary conditions. The energy is calculated with the modified neglect of differential overlap method,¹³ which is a semiempirical electronic structure method; all calculations are carried out with the MOPAC software program.¹⁴ The potential energy is minimized with respect to the atomic positions, with the simulation cell fixed.¹⁵ The volume of the simulation cell is then reduced isotropically in small increments ($<0.3\%$). After each volume change, the potential energy is re-minimized with respect to the atomic coordinates (at constant volume), starting from the atomic coordinates at the previous volume. The normal-mode frequencies are calculated at the energy minimum, and the pressure is obtained numerically from the derivative of the energy (at the minimum) with respect to volume.

The results for the pressure as the glass is compressed are shown in Fig. 2. The zero pressure density is 2.18 g/cm^3 , which is in good agreement with the experimental value¹⁶ of

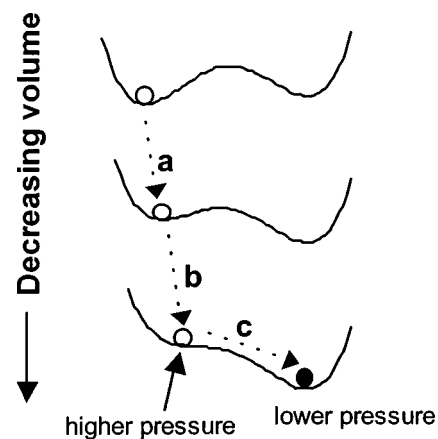


FIG. 1. Schematic of a pressure-induced disappearance of an energy minimum. The curves represent the potential energy along the relevant coordinate, and the circles represent the state of the system. The change in the state of the system denoted by arrow “c” corresponds to the structural rearrangement associated with the mechanical instability.

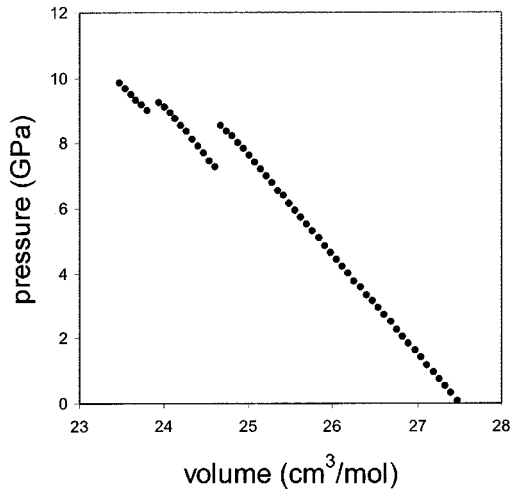


FIG. 2. Pressure as a function of volume.

2.20 g/cm³. The bulk modulus is 82 GPa (calculated from the derivative of pressure with respect to volume), which is significantly higher than the experimental value¹⁷ of 37 GPa; this difference is not a problem because the purpose of the present investigation is to see if the mechanical instabilities found previously in force field calculations also occur in electronic structure calculations, rather than to make quantitative comparison to experiment.

The pressure usually increases continuously with decreasing volume (see Fig. 2), but discontinuous pressure drops occur twice in the volume range examined—at $V=24.7$ and 23.9 cm³/mol. The origin of these discontinuous pressure drops becomes evident from an examination of the volume dependence of the normal-mode frequencies, shown in Fig. 3. The discontinuous pressure drops occur when the lowest normal-mode frequency of the system decreases to zero. The normal-mode frequencies are proportional to the square root of the curvature of the energy minimum in orthogonal directions, and thus the decrease of a normal-mode frequency to zero implies that the energy minimum flattens out until it disappears, as shown in Fig. 1. After the energy minimum disappears, the system is mechanically unstable (i.e., no energy barrier exists) and it relaxes to an alternate potential-

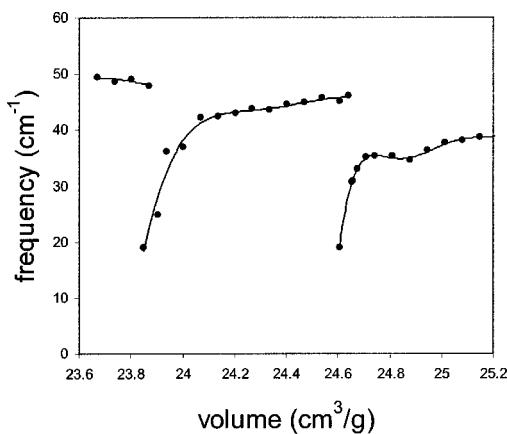
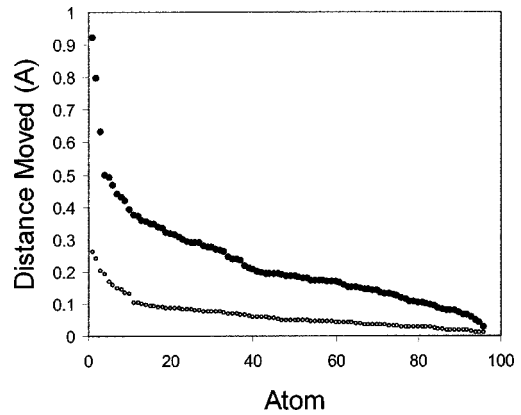


FIG. 3. Lowest normal-mode frequency as a function of volume. Lines are a guide to the eye.

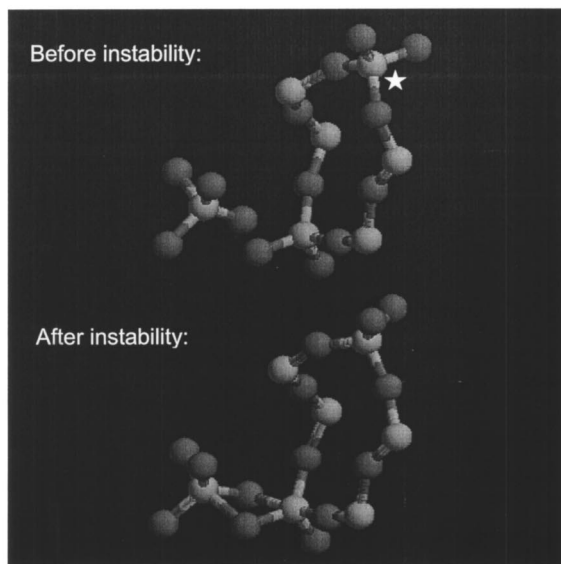
FIG. 4. Distance moved by each atom (with respect to the center of mass) following the mechanical instabilities. Filled circles: instability at $V=24.7$ cm³/mol. Open circles: $V=23.9$ cm³/mol.

energy minimum that has a lower pressure.

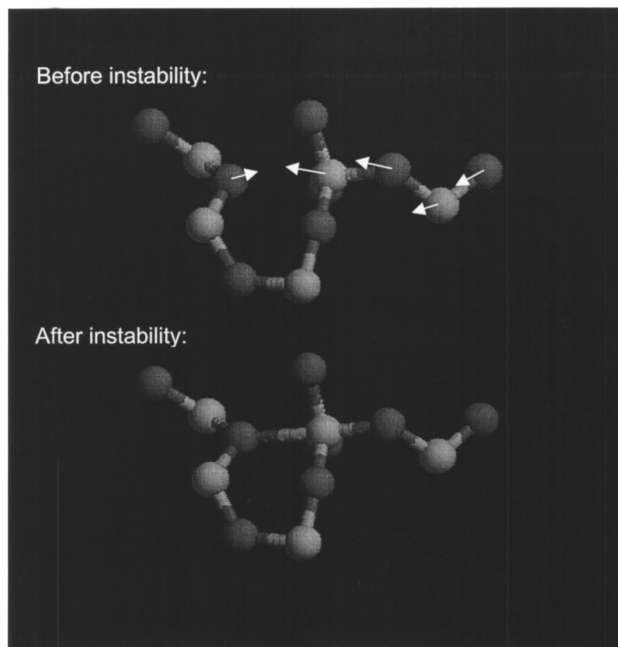
The structural changes that follow the disappearance of energy minima are localized to a small number of atoms, as shown in Fig. 4. Even though all atoms move to some extent, a small number of atoms (of order 10) move a significantly larger amount than the rest. A quantitative (but arbitrary) measure of the number of atoms involved in the structural change is the participation number $p = \sum_{i=1}^{N_{\text{atoms}}} (d_i/d_{\text{max}})^2$, where d_i is the distance moved (with respect to the center of mass) by atom i , and d_{max} is the largest displacement undergone by any one atom;¹⁸ $p=1$ indicates that only one atom moves, and $p=N_{\text{atoms}}$ indicates that all atoms move equally. The participation number $p=8.3$ is for the instability at $V=24.7$ cm³/mol and $p=9.1$ is for the instability at $V=23.9$ cm³/mol. These structural rearrangements can be considered as the significant movement of a small group of atoms (of order 10), plus an elastic relaxation of a larger group of surrounding atoms in response to changes of the small group (for the small system size examined here, all of the other atoms in the system belong to this larger group, which undergoes elastic relaxation).

The large discontinuities in the system's pressure-volume curve are due to the small system size. As the number of atoms in the system increases towards the macroscopic limit, the mechanical instabilities occur more frequently (because there are more groups of atoms that can undergo instabilities), while the discontinuous drops in the pressure decrease in magnitude (because a decreasing fraction of the system is involved in the localized instability).¹⁹ In the macroscopic limit, the changes in pressure with volume will be continuous, even though the mechanical instabilities remain the mechanism for structural change.

These results based on electronic structure calculations are qualitatively the same as our previous results based on force field calculations.⁸⁻¹⁰ Both sets of results lead to the conclusion that pressure-induced structural transformations occur in silica glass via localized mechanical instabilities (at low temperature; room temperature is considered "low"). This conclusion appears to be independent of the methodology of the energy calculation, as it arises from both force field calculations and electronic structure calculations. The



(a)



(b)

FIG. 5. Relevant atomic positions before and after the mechanical instabilities. Note the changes in short-range order (ion coordination) and intermediate-range order (ring size distribution). (a) Instability at $V=24.7 \text{ cm}^3/\text{mol}$. (b) $V=23.9 \text{ cm}^3/\text{mol}$. See text for the significance of the star in (a) and the arrows in (b).

relationship between these mechanical instabilities and the transformations of silica under pressure are discussed elsewhere.^{8,9}

The nature of the structural rearrangements that accompany the mechanical instabilities are examined in more detail in this paper. Although the changes in short-range order have also been addressed previously,⁸ the changes in intermediate-range order and the cooperative nature of the rearrangements have not yet been addressed, to our best knowledge.

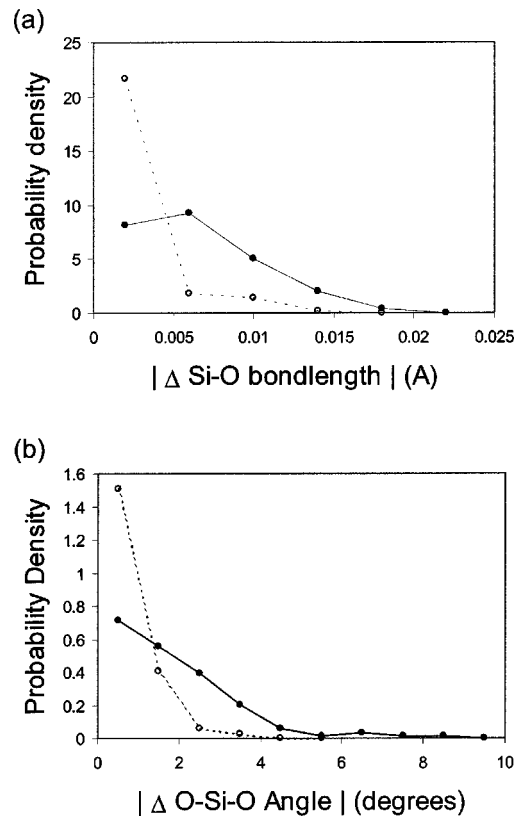


FIG. 6. Changes in intratetrahedral properties following mechanical instabilities. (a) Bond lengths; (b) intratetrahedral bond angles. Filled circles and solid lines: instability at $V=24.7 \text{ cm}^3/\text{mol}$. Open circles and dashed lines: $V=23.9 \text{ cm}^3/\text{mol}$. These results include only silicon ions that have fourfold coordination both before and after the instability.

The changes in short-range order caused by the mechanical instabilities correspond to increases in the ion coordination.⁸ As shown in Fig. 5, the instability at $V=24.7 \text{ cm}^3/\text{mol}$ causes the coordination of two neighboring silicon ions to increase from four to five, and the instability at $V=23.9 \text{ cm}^3/\text{mol}$ causes the coordination of one silicon ion to increase from four to five (an Si-O pair is considered bonded if the Si-O distance is $<2.2 \text{ \AA}$; in all three coordination changes observed here, the relevant Si-O distances change from ~ 2.5 to $\sim 2.0 \text{ \AA}$). The increase in ion coordination with increasing pressure agrees with experiment.⁴⁻⁶

Intermediate-range order can be described in part by the ring size distribution. A ring is defined as the shortest closed loop of Si-O units that leaves an initial silicon ion via one Si-O unit and returns to the initial silicon ion via a different Si-O unit; the size of the ring is the number of Si-O units in the ring. The average ring size in amorphous silica is ~ 6 .²⁰ The present results show that pressure-induced mechanical instabilities lead to the formation of small rings, and thus a shift in the ring size distribution to smaller ring sizes: As shown in Fig. 5, the instability at $V=24.7 \text{ cm}^3/\text{mol}$ involves the formation of a two-membered ring, and the instability at $V=23.9 \text{ cm}^3/\text{mol}$ involves the formation of a three-membered ring. The pressure-induced shift to smaller ring sizes agrees with experiment.⁴

The structural rearrangements associated with the instabilities involve highly cooperative motion. As shown in Fig. 6, the changes in the SiO_4 tetrahedra are very small, with all bond lengths changing by $<0.02 \text{ \AA}$, and almost all intratetrahedral angles changing by $<4^\circ$ (for comparison, the standard deviations of the bond lengths and intratetrahedral angles are 0.015 \AA and 6° , respectively). These small changes in the SiO_4 tetrahedra are surprising because the ions move significantly larger distances (see Fig. 4). As a particular example, consider the SiO_4 tetrahedron denoted by the star in Fig. 5(a). Even though the four oxygen ions in this tetrahedron move distances ranging from 0.49 to 0.91 \AA while the silicon ion moves 0.09 \AA , the average magnitudes of the changes in the bond lengths and intratetrahedral angles are only 0.008 \AA and 1.4° , respectively—the net effect of these atomic displacements is that the tetrahedron undergoes a large rotation ($\sim 25^\circ$) and a translation, with very little

internal distortion [see Fig. 5(a)]. Thus the structural rearrangements associated with the instabilities correspond to rigid unit modes (RUM's), in which the SiO_4 tetrahedra rotate and translate as nearly rigid units. Previous work has shown that RUM's play important roles in the thermally activated dynamics of both crystalline and amorphous silicates.^{12,21}

Furthermore, the structural rearrangement associated with the instability at $V=23.9 \text{ cm}^3/\text{mol}$ corresponds to motion in which the cooperatively rearranging region is not compact but, rather, “stringlike.” This result is shown in Fig. 5(b) where the arrows show the movement of the five ions with the largest displacements. Such stringlike motion has been found for thermally activated dynamics in supercooled Lennard-Jones liquids.²²

Funding for this project was provided by NSF Grant No. DMR-0080191.

-
- ¹P. W. Bridgman and I. Simon, *J. Appl. Phys.* **24**, 405 (1953).
²M. Grimsditch, *Phys. Rev. Lett.* **52**, 2379 (1984).
³C.-S. Zha, R. J. Hemley, H.-K. Mao, T. S. Duffy, and C. Meade, *Phys. Rev. B* **50**, 13 105 (1994).
⁴R. J. Hemley, H. K. Mao, P. M. Bell, and B. O. Mysen, *Phys. Rev. Lett.* **57**, 747 (1986).
⁵Q. Williams and R. Jeanloz, *Science* **239**, 902 (1988).
⁶C. Meade, R. J. Hemley, and H. K. Mao, *Phys. Rev. Lett.* **69**, 1387 (1992).
⁷V. G. Karpov and M. Grimsditch, *Phys. Rev. B* **48**, 6941 (1993).
⁸D. J. Lacks, *Phys. Rev. Lett.* **80**, 5385 (1998).
⁹D. J. Lacks, *Phys. Rev. Lett.* **84**, 4629 (2000).
¹⁰M. M. Roberts, J. R. Wienhoff, K. Grant, and D. J. Lacks, *J. Non-Cryst. Solids* **281**, 205 (2001).
¹¹J. D. MacKenzie, *J. Am. Ceram. Soc.* **47**, 76 (1964).
¹²K. Trachenko, M. T. Dove, K. D. Hammonds, M. J. Harris, and V. Heine, *Phys. Rev. Lett.* **81**, 3431 (1998).
¹³M. J. S. Dewar and W. Thiel, *J. Am. Chem. Soc.* **99**, 4899 (1977); M. J. S. Dewar, J. Friedheim, G. Grady, E. F. Healy and J. J. P. Stewart, *Organometallics* **5**, 375 (1986).
¹⁴Computer code MOPAC 2000, (Schrodinger, Inc., New York, 1999).
¹⁵The initial atomic positions were generated by molecular-dynamics simulations using the force field of S. Tsuneyuki, M. Tsukada, H. Aoki, and Y. Matsui, *Phys. Rev. Lett.* **61**, 869 (1988). A glass is formed in these simulations by cooling an SiO_2 liquid with several stages of constant-temperature molecular-dynamics simulations.
¹⁶R. L. Mozzi and B. E. Warren, *J. Appl. Crystallogr.* **2**, 164 (1969).
¹⁷K. Kondo, S. Iio, and A. Sawaoko, *J. Appl. Phys.* **52**, 2826 (1981).
¹⁸A. Heuer and R. J. Silbey, *Phys. Rev. Lett.* **70**, 3911 (1993).
¹⁹D. L. Malandro and D. J. Lacks, *J. Chem. Phys.* **110**, 4593 (1999).
²⁰J. P. Rino, I. Ebbsjo, R. K. Kalia, A. Nakano, and P. Vashishta, *Phys. Rev. B* **47**, 3053 (1993).
²¹M. T. Dove, M. J. Harris, A. C. Hannon, J. M. Parker, I. P. Swainson, and M. Gambhir, *Phys. Rev. Lett.* **78**, 1070 (1997).
²²C. Donati, J. F. Douglas, W. Kob, S. J. Plimpton, P. H. Poole, and S. C. Glotzer, *Phys. Rev. Lett.* **80**, 2338 (1998).